Microsomal Activation of Dibenzo[*def,mno*]chrysene (Anthanthrene), a Hexacyclic Aromatic Hydrocarbon without a Bay-Region, to Mutagenic Metabolites

Karl L. Platt,* Christian Degenhardt, Stefanie Grupe, Heinz Frank,‡ and Albrecht Seidel‡

Institute of Toxicology, University of Mainz, Obere Zahlbacher Strasse 67, D-55131 Mainz, Germany

Received August 8, 2001

Metabolically formed dihydrodiol epoxides in the bay-region of polycyclic aromatic hydrocarbons are thought to be responsible for the genotoxic properties of these environmental pollutants. The hexacyclic aromatic hydrocarbon dibenzo[*def,mno*]chrysene (anthanthrene), although lacking this structural feature, was found to exhibit considerable bacterial mutagenicity in histidine-dependent strains TA97, TA98, TA100, and TA104 of *S. typhimurium* in the range of 18−40 his$^+$-revertant colonies/nmol after metabolic activation with the hepatic postmitochondrial fraction of Sprague−Dawley rats treated with Aroclor 1254. This mutagenic effect amounted to 44−84% of the values determined with benzo[*a*]pyrene under the same conditions. The specific mutagenicity of anthanthrene in strain TA100 obtained with the cell fraction of untreated animals was 6 his$^+$-revertant colonies/nmol and increased 2.7-fold after treatment with phenobarbital and 4.5-fold after treatment with 3-methylcholanthrene. To elucidate the metabolic pathways leading to genotoxic metabolites, the microsomal biotransformation of anthanthrene was investigated. A combination of chromatographic, spectroscopic, and biochemical methods allowed the identification of the *trans*-4,5-dihydrodiol, 4,5-oxide, 4,5-, 1,6-, 3,6-, and 6,12-quinones, and 1- and 3-phenols. Furthermore, two diphenols derived from the 3-phenol, possibly the 3,6 and 3,9 positional isomers, as well as two phenol dihydrodiols were isolated. Three pathways of microsomal biotransformation of anthanthrene could be distinguished: The K-region metabolites are formed via pathway I dominated by monooxygenases of the P450 1B subfamily. On pathway II the polynuclear quinones of anthanthrene are formed. Pathway III is preferentially catalyzed by monooxygenases of the P450 1A subfamily and leads to the mono- and diphenols of anthanthrene. The K-region oxide and the 3-phenol are the only metabolites of anthanthrene with strong intrinsic mutagenicity, qualifying them as ultimate mutagens or their precursors. From the intrinsic mutagenicity of these two metabolites and their metabolic formation, the maximal mutagenic effect was calculated. This demonstrates the dominating role of pathway III in the mutagenicity of anthanthrene under conditions where it exhibits the strongest bacterial mutagenicity.

Introduction

The class of the polycyclic aromatic hydrocarbons (PAH),[1] ubiquitously present in the environment as the result of incomplete combustion of organic matter, contains a great number of strong carcinogens. As PAH are not genotoxic by themselves, they need enzymatic transformation to reactive metabolites. A characteristic structural feature of most carcinogenic PAH is the presence of a sterically hindered bay-region (cf. Scheme 1) which is involved in the metabolic activation to dihydrodiol epoxides considered to be ultimate carcinogenic metabolites of PAH (*1*). Other pathways of metabolic activation include enzymatic conversion to radical cations (*2*), methylated derivatives (*3*), *o*-quinones (*4*), or ring-opened metabolites (*5*, *6*), all of which could finally lead to DNA modifications, but their relationship to the carcinogenicity of PAH is less clear. These alternative activation mechanisms can best be studied in genotoxic PAH

Scheme 1. Structural Formulas, Molecular Regions, and Numbering of Benzo[*a*]pyrene and Dibenzo[*def,mno*]chrysene (Anthanthrene)

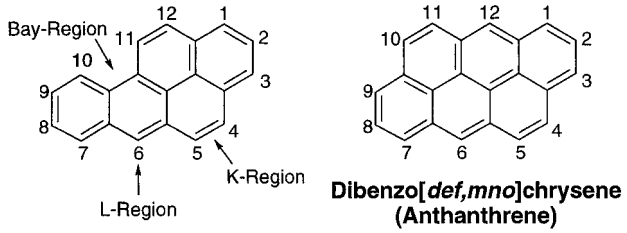

* To whom correspondence should be addressed. E-mail: platt@mail.uni-mainz.de.

‡ Biochemical Institute for Environmental Carcinogens, Prof. Dr. Gernot Grimmer-Foundation, Lurup 4, D-22927 Grosshansdorf, Germany.

[1] Abbreviations: anthanthrene, dibenzo[*def,mno*]chrysene; 4,5-dihydrodiol, *trans*-4,5-dihydroxy-4,5-dihydroanthanthrene; EtOH, ethanol; 4,5-oxide, 4,5-epoxy-4,5-dihydroanthanthrene; 1-phenol, 1-hydroxyanthanthrene (other phenols are similarly designated); MeOH, methanol; 4,5-quinone, anthanthrene 4,5-quinone (other quinones are similarly designated); PAH, polycyclic aromatic hydrocarbon(s); PAPS, adenosine 3′-phosphate 5′-phosphosulfate; TCPO, 1,1,1-trichloro-2-propene oxide; UDPAG, uridine 5′-diphospho-*N*-acetylglucosamine; UDPGA, uridine 5′-diphosphoglucuronic acid.

10.1021/tx010131t CCC: $22.00
Published on Web 02/06/2002

lacking a bay-region: The hexacyclic aromatic hydrocarbon dibenzo[*def*,*mno*]chrysene (anthanthrene), where the bay-region of benzo[*a*]pyrene is bridged by an additional aromatic ring (Scheme 1), is such an example. Anthanthrene occurs in relatively high concentration in coal-tar and in all environmental samples containing PAH (*7*). Anthanthrene was found to be mutagenic in bacterial short-term tests (*8*−*11*). It exhibited skin carcinogenicity after long-term topical application (*12*) or by employing the initiation−promotion protocol to mice (*13*) as well as lung carcinogenicity after pulmonal implantation in rats (*14*), while in several other in vivo studies anthanthrene did not show any carcinogenic activity (*7*). Hence, after evaluation of the experimental data, the International Agency for Research on Cancer concluded that '*there is limited evidence that anthanthrene is carcinogenic to experimental animals*' while the evidence for its mutagenicity is characterized as '*inadequate*' (*7*).

We, therefore, wished (i) to study the bacterial mutagenicity of anthanthrene in more detail and investigate its enzymatic control as well as (ii) to elucidate its hitherto unknown biotransformation in order to reveal the metabolic pathway(s) leading to genotoxicity.

Experimental Procedures

Chemicals. 3-Methylcholanthrene, the methoxy tetralones, and also reagents for the synthetic procedures were supplied by Sigma-Aldrich (Taufkirchen, Germany). Aroclor 1254 was obtained from Bayer (Leverkusen, Germany), sodium phenobarbital from Synopharm (Barsbuettel, Germany), trioctanoin from Sigma (Taufkirchen, Germany), and 1,1,1-trichloro-2-propene oxide (TCPO) from EGA (Steinheim, Germany). Biochemicals were from Roche Diagnostics (Mannheim, Germany); solvents for HPLC were from Baker (Gross-Gerau, Germany); all other chemicals of analytical grade were purchased from Merck (Darmstadt, Germany).

Synthesis of Anthanthrene. Anthanthrene was obtained (*15*) by a zinc dust melt from the commercially available 6,12-quinone (TCI, Tokyo, Japan) after purification in benzene over Florisil (60−100 mesh, Promochem, Wesel, Germany) and twice recrystallization from toluene in 39% yield and 99% purity (HPLC: LiChrospher RP18, 5 μm, 4 × 250 mm; 100% MeOH, 0.8 mL/min): mp >250 °C [lit.: 264 °C (*16*)]; ^{1}H NMR (CD_2Cl_2) δ 8.82 (s, 2H, $H_{6,12}$), 8.56 (d, 2H, $H_{1,7}$, $J_{1,2} = J_{7,8} = 8.1$ Hz), 8.24 (d, 2H, $H_{3,9}$, $J_{2,3} = J_{8,9} = 6.9$ Hz), 8.18 (d, 2H, $H_{5,11}$, $J_{4,5} = J_{10,11} = 9.1$ Hz), 8.16 (pseudo-t, 2H, $H_{2,8}$), 8.10 (d, 2H, $H_{4,10}$); UV/vis (EtOH) λ_{max} (nm) (ϵ [M^{-1} cm^{-1}]): 210 (36 200), 232 (82 200), 258 (33 700), 293 (36 400), 306 (69 700), 381 (10 900), 400 (25 800), 405 (28 000), 421 (35 000), 429 (48 700); EI-MS *m*/*z* (rel intensity, %) 277 (23) $[MH]^+$, 276 (100) $[M]^+$, 138 (28) $[M]^{2+}$.

For the preparation of [G-^{3}H]anthanthrene by tritium exchange (Amersham Buchler, Braunschweig, Germany), the parent hydrocarbon was dissolved in dioxane and treated with ^3H_2O (925−1850 GBq [25−50 Ci]/mmol) in the presence of an Al/Rh catalyst. After removal of labile tritium, the raw product (specific activity, 174 GBq [4.7 Ci]/mmol) was dissolved in toluene and kept at −20 °C. The tritium distribution within the anthanthrene molecule was determined from the tritium NMR spectrum: ^{3}H NMR ($CDCl_3$, 41 800 scans) δ 8.87 (s, 2H, $H_{6,12}$), 8.61 (s, 2H, $H_{1,7}$), 8.29 (s, 2H, $H_{3,9}$), 8.23 (s, 2H, $H_{5,11}$), 8.21 (s, 2H, $H_{2,8}$), 8.15 (s, 2H, $H_{4,10}$). Integration of the signals indicated a rather uniform tritium distribution with 25.1% at $H_{2,8}$, 19.0% at $H_{4,10}$, 15.7% at $H_{5,11}$, 14.1% at $H_{6,12}$, 13.4% at $H_{1,7}$, and 12.7% at $H_{3,9}$.

Prior to use as substrate in microsomal incubations, an aliquot of the stock solution was evaporated, and the crude product was dissolved in Me_2SO (50 μL) and purified by HPLC [stationary phase as above; mobile phase: linear gradient of 65% (v/v) aqueous MeOH to 100% MeOH within 50 min; flow rate: 0.8 mL/min]. The fraction of the eluate containing anthanthrene was collected and brought to dryness with a stream of N_2, resulting in a radiochemical purity of 98%.

Synthesis of Polynuclear Quinones of Anthanthrene. The three polynuclear quinones of anthanthrene were synthesized by oxidation of the parent hydrocarbon with sodium dichromate (*17*). Subsequent separation of the crude mixture was achieved on Florisil by sequential elution with toluene/ethyl acetate (98:2, then 9:1, v/v) and chloroform/acetone (9:1, v/v). Several fractions were obtained with enriched mixtures of anthanthrene 6,12-, 3,6- and 1,6-quinone (eluting in this order) representing an overall yield of 87%. The pure isomers were obtained by several rechromatographic steps (HPLC: LiChrospher RP18, 5 μm, 4 × 250 mm; 100% MeOH, 1.0 mL/min).

(1) Anthanthrene 6,12-quinone: ^{1}H NMR (THF-d_8) δ 8.73 (d, 2H, $H_{1,7}$, $J_{1,2} = J_{7,8} = 7.4$ Hz), 8.73 (d, 2H, $H_{5,11}$, $J_{4,5} = J_{10,11} = 8.6$ Hz), 8.38 (d, 2H, $H_{3,9}$, $J_{2,3} = J_{8,9} = 7.4$ Hz), 8.25 (d, 2H, $H_{4,10}$), 7.94 (pseudo-t, 2H, $H_{2,8}$); UV/vis (EtOH) λ_{max} (nm) (ϵ [M^{-1} cm^{-1}]): 225 (21 800), 274 (16 500), 354 (6600), 446 (4400), 472 (5000); EI-MS *m*/*z* (rel intensity, %) 307 (24) $[MH]^+$, 306 (100) $[M]^+$, 278 (15) $[M - CO]^+$, 250 (17) $[M - 2 \times CO]^+$.

(2) Anthanthrene 3,6-quinone: ^{1}H NMR (CD_2Cl_2) δ 8.87 (d, 1H, H_5, $J_{4,5} = 7.8$ Hz), 8.76 (dd, 1H, H_7, $J_{7,8} = 6.2$ Hz, $J_{7,9} = 1.2$ Hz), 8.69 (d, 1H, H_4), 8.33 (d, 1H, H_9, $J_{8,9} = 8.0$ Hz), 8.19 (s, 1H, H_{12}), 8.10 (AB-system, 2H, $H_{10,11}$, $J_{10,11} = 8.6$ Hz), 7.91 (pseudo-t, 1H, H_8), 7.90 (d, 1H, H_1, $J_{1,2} = 9,9$ Hz), 6.75 (d, 1H, H_2); UV/vis (MeOH) λ_{max} (nm) (ϵ [M^{-1} cm^{-1}]): 207 (47 900), 246 (20 400), 331 (18 400), 470 (5300); EI-MS *m*/*z* (rel intensity, %) 307 (27) $[MH]^+$, 306 (100) $[M]^+$, 278 (47) $[M - CO]^+$, 250 (33) $[M - 2 \times CO]^+$.

(3) Anthanthrene 1,6-quinone: ^{1}H NMR (THF-d_8) δ 9.05 (s, 1H, H_{12}), 8.77 (d, 1H, H_5, $J_{4,5} = 7.6$ Hz), 8.76 (dd, 1H, H_7, $J_{7,8} = 7.3$ Hz, $J_{7,9} = 1.2$ Hz), 8.44 (dd, 1H, H_9, $J_{8,9} = 7.9$ Hz), 8.30 (AB-system, 2H, $H_{10,11}$, $J_{10,11} = 8.8$ Hz), 8.10 (d, 1H, H_4), 7.98 (pseudo-t, 1H, H_8), 7.96 (d, 1H, H_3, $J_{2,3} = 9.8$ Hz), 6.75 (d, 1H, H_2); UV/vis (MeOH) λ_{max} (nm) (ϵ [M^{-1} cm^{-1}]): 207 (43 600), 310 (7100), 322 (7600), 434 (5700); EI-MS *m*/*z* (rel intensity) 307 (27) $[MH]^+$, 306 (100) $[M]^+$, 278 (33) $[M - CO]^+$, 250 (28) $[M - 2 \times CO]^+$.

Synthesis of the K-Region Derivatives of Anthanthrene. Anthanthrene was converted to the 4,5-osmate ester, hydrolyzed to the *cis*-4,5-dihydrodiol, and oxidized with 2,3-dichloro-5,6-dicyano-*p*-benzoquinone (*18*), yielding anthanthrene 4,5-quinone (11%): mp >250 °C; ^{1}H NMR ($CDCl_3$) δ 8.90 (s, 1H, H_6), 8.61 (dd, 1H, H_3, $J_{2,3} = 7.2$ Hz, $J_{1,3} = 1.2$ Hz), 8.42 (dd, 1H, H_1, $J_{1,2} = 8.2$ Hz, $J_{1,3} = 0.8$ Hz), 8.34 (s, 1H, H_{12}), 8.20 (d, 1H, H_7, $J_{7,8} = 7.7$ Hz), 8.11 (d, 1H, H_9, $J_{8,9} = 7.0$ Hz), 7.95 (pseudo-t, 1H, H_8), 7.79−7.86 (m, 3H, H_2, H_{10}, H_{11}); UV/vis (EtOH) λ_{max} (nm) (ϵ [M^{-1} cm^{-1}]): 204 (37 100), 250 (54 400), 285 (42 100), 381 (14 800), 401 (15 600); EI-MS *m*/*z* (rel intensity, %) 307 (21) $[MH]^+$, 306 (81) $[M]^+$, 279 (24) $[MH - CO]^+$, 278 (100) $[M - CO]^+$, 250 (36) $[M - 2 \times CO]^+$.

The 4,5-quinone was reduced with $NaBH_4$ in EtOH in the presence of oxygen (*19*) to *trans*-4,5-dihydroxy-4,5-dihydroanthanthrene (70%): mp 222−224 °C (dec); ^{1}H NMR (acetone-d_6/Me_2SO-d_6) δ 8.67 (s, 1H, H_{12}), 8.57 (s, 1H, H_6), 8.37 (d, 1H, H_7, $J_{7,8} = 7.6$ Hz), 8.27 (d, 1H, H_9, $J_{8,9} = 8.2$ Hz), 8.18 (d, 1H, H_1, $J_{1,2} = 7.2$ Hz), 8.08 (AB-system, 2H, $H_{10,11}$, $J_{10,11} = 9.2$ Hz), 8.06−8.02 (m, 2H, $H_{3,8}$), 7.84 (dd, 1H, H_2, $J_{2,3} = 8.1$ Hz), 5.21 (d, 1H, H_4, $J_{4,5} = 9.6$ Hz), 5.17 (d, 1H, H_5); UV/vis (EtOH) λ_{max} (nm) (ϵ [M^{-1} cm^{-1}]): 212 (27 900), 232 (44 200), 266 (37 100), 291 (38 700), 303 (46 400), 349 (11 000), 367 (22 000), 388 (25 400); EI-MS *m*/*z* (rel intensity, %) 311 (27) $[MH]^+$, 310 (100) $[M]^+$.

The *trans*-4,5-dihydrodiol was cyclized with the dimethyl acetal of dimethylformamide (*20*), furnishing anthanthrene 4,5-oxide (47%): mp 185 °C (dec); ^{1}H NMR ($CDCl_3$) δ 8.56 (s, 1H, H_6), 8.54 (s, 1H, H_{12}), 8.30 (d, 1H, H_7 or H_9, $J = 8.0$ Hz), 8.28 (d, 1H, H_9 or H_7, $J = 7.7$ Hz), 8.12 (d, 1H, H_1, $J_{1,2} = 7.5$ Hz), 8.04 (d, 1H, H_3, $J_{2,3} = 7.3$ Hz), 8.01 (pseudo-t, 1H, H_8), 7.96 (AB-system, 2H, $H_{10,11}$, $J_{10,11} = 9.1$ Hz), 7.80 (pseudo-t, 1H, H_2), 5.02 (d, 1H, H_4, $J_{4,5} = 3.8$ Hz), 4.94 (d, 1H, H_5); UV/vis (MeOH) λ_{max}

(nm) (ϵ_{rel}): 227 (0.81), 264 (0.76), 288 (0.82), 299 (1.00), 367 (0.46), 386 (0.53), 408 (0.05); EI-MS *m/z* (rel intensity, %) 293 (24) $[MH]^+$, 292 (100) $[M]^+$, 263 (42) $[M - CHO]^+$.

Synthesis of the L-Region Derivatives of Anthanthrene. Vilsmeier formylation of anthanthrene according to Buu-Hoi and Lavit (*21*) yielded the 6-aldehyde (45%) which was reduced with $NaBH_4$ to 6-hydroxymethylanthanthrene (93%): mp 212 °C (dec); ^{1}H NMR (acetone-d_6/Me_2SO-d_6) δ 9.08 (d, 1H, H_7, $J_{7,8}$ = 8.3 Hz), 9.00 (s, 1H, H_{12}), 8.74 (d, 1H, H_5, $J_{4,5}$ = 9.5 Hz), 8.66 (d, 1H, H_9, $J_{8,9}$ = 8.0 Hz), 8.39−8.36 (m, 2H, $H_{1,3}$), 8.30−8.20 (m, 5H, $H_{2,4,8,10,11}$), 8.06−8.02 (m, 2H, $H_{3,8}$), 7.84 (dd, 1H, H_2, $J_{2,3}$ = 8.1 Hz), 5.21 (d, 1H, H_4, $J_{4,5}$ = 9.6 Hz), 5.81 (s, 2H, $-CH_2-$); UV/vis (EtOH) λ_{max} (nm) (ϵ $[M^{-1}\ cm^{-1}]$): 211 (33 600), 234 (72 300), 258 (29 200), 296 (34 600), 308 (71 100), 388 (10 900), 412 (30 000), 424 (19 600), 436 (54 700); EI-MS *m/z* (rel intensity, %) 307 (25) $[MH]^+$, 306 (100) $[M]^+$, 289 (80) $[MH - H_2O]^+$, 288 (9) $[M - H_2O]^+$, 287 (23) $[M - H_2O - H]^+$, 275 (24) $[MH - CH_3OH]^+$, 274 (28) $[M - CH_3OH]^+$.

Wolff−Kishner reduction of 6-formylanthanthrene afforded 6-methylanthanthrene (83%): mp 184 °C [lit.: 192 °C (*21*)]; ^{1}H NMR ($CDCl_3$) δ 8.74 (dd, 1H, H_7, $J_{7,8}$ = 8.2 Hz, $J_{7,9}$ = 0.9 Hz), 8.72 (s, 1H, H_{12}), 8.48 (d, 1H, H_9, $J_{8,9}$ = 7.9 Hz), 8.45 (d, 1H, H_5, $J_{4,5}$ = 9.5 Hz), 8.22−8.04 (m, 7H, $H_{1,2,3,4,6,8,11}$), 3.35 (s, 3H, $-CH_3$); UV/vis (EtOH) λ_{max} (nm) (ϵ $[M^{-1}\ cm^{-1}]$): 211 (31 200), 234 (61 900), 258 (26 800), 296 (30 000), 308 (39 300), 389 (9500), 412 (23 500), 437 (32 300); EI-MS *m/z* (rel intensity, %) 291 (24) $[MH]^+$, 290 (100) $[M]^+$.

Synthesis of Non-K-Region Phenols of Anthanthrene. The synthesis of 1-hydroxy-, 2-hydroxy-, and 3-hydroxyanthanthrene (Supporting Information: Scheme S1) will be published in full detail elsewhere. In brief, 1-hydroxyanthanthrene was prepared from 5-methoxy-1-tetralone that was subjected to a Reformatsky reaction with ethyl bromoacetate, followed by dehydration, aromatization, and hydrolysis, resulting in 5-methoxy-1-naphthylacetic acid. This compound was converted with methyl 3-formylbenzoate via a Perkin reaction to α-(5-methoxy-1-naphthyl)-3-methoxycarbonylcinnamic acid which was transformed to its methyl ester. Oxidative photocyclization (*22*, *23*) led to a mixture of 5,8-bismethoxycarbonyl- and 5,10-bismethoxycarbonyl-1-methoxychrysene, the former being much less soluble in MeOH than the latter. Thus, a considerable enrichment of 5,10-bismethoxycarbonyl-1-methoxychrysene was achieved by rinsing the crude mixture with MeOH. Subsequent chromatography on silica gel eluting with $CHCl_3$ yielded pure 5,10-bismethoxycarbonyl-1-methoxychrysene which was reduced to the benzylic alcohol with $LiAlH_4$. 5,10-Bishydroxymethyl-1-methoxychrysene was converted by oxidation with pyridinium dichromate to 5,10-diformyl-1-methoxychrysene. This aldehyde was reacted under phase-transfer conditions with trimethylsulfonium iodide to furnish 5,10-bisepoxyethyl-1-methoxychrysene. Treatment of this bisoxiranyl compound with boron trifluoride etherate (*24*) resulted in the formation of 1-methoxyanthanthrene. Cleavage of the methoxy group with boron tribromide furnished 1-hydroxyanthanthrene (overall yield 0.5%): ^{1}H NMR (acetone-d_6) δ 9.18 (s, 1H, H_{12}), 8.76 (s, 1H, H_6), 8.52 (d, 1H, H_7, $J_{7,8}$ = 7.8 Hz), 8.25 (d, 1H, H_4, $J_{4,5}$ = 9.3 Hz), 8.22 (d, 1H, H_9, $J_{8,9}$ = 7.2 Hz), 8.15 (d, 1H, H_3, $J_{2,3}$ = 8.0 Hz), 8.13 (pseudo-t, 1H, H_8), 8.12 (d, 1H, H_5), 8.01 (AB-system, 2H, $H_{10,11}$, $J_{10,11}$ = 9.2 Hz), 7.70 (d, 1H, H_2, $J_{2,3}$ = 8.0 Hz); UV/vis (MeOH) λ_{max} (nm) (ϵ_{rel}): 213 (0.84), 233 (1.00), 312 (0.86), 405 (0.31), 430 (0.40), 450 (0.39).

2-Hydroxyanthanthrene was prepared according to the synthetic pathway described above utilizing 6-methoxy-1-tetralone as starting material (overall yield 2.0%): mp 228−230 °C (dec); ^{1}H NMR (acetone-d_6/Me_2SO-d_6) δ 8.92 (s, 1H, H_6 or H_{12}), 8.78 (s, 1H, H_{12} or H_6), 8.60 (d, 1H, H_7, $J_{7,8}$ = 8.0 Hz), 8.30 (d, 1H, H_9, $J_{8,9}$ = 7.2 Hz), 8.18 (AB-system, 2H, $H_{10,11}$, $J_{10,11}$ = 9.2 Hz), 8.16 (AB-system, 2H, $H_{4,5}$, $J_{4,5}$ = 9.2 Hz), 8.15 (pseudo-t, 1H, H_8), 7.99 (d, 1H, H_1 or H_3, J = 2.1 Hz), 7.87 (d, 1H, H_3 or H_1, J = 2.1 Hz); UV/vis (EtOH) λ_{max} (nm) (ϵ $[M^{-1}\ cm^{-1}]$): 213 (35 900), 236 (49 100), 269 (29 200), 295 (29 400), 309 (23 500), 321 (22 400), 410 (19 500), 425 (21 200), 440 (15 900); EI-MS *m/z* (rel intensity, %) 293 (24) $[MH]^+$, 292 (100) $[M]^+$, 263 (36) $[M - CHO]^+$.

3-Hydroxyanthanthrene was prepared according to the synthetic pathway described above utilizing 7-methoxy-1-tetralone as starting material (overall yield 0.5%): mp >250 °C; ^{1}H NMR (acetone-d_6) δ 9.78 (s, 1H, OH), 8.81 (s, 1H, H_6 or H_{12}), 8.75 (s, 1H, H_{12} or H_6), 8.53−8.48 (m, 2H, $H_{1,7}$), 8.42 (d, 1H, H_9, $J_{8,9}$ = 9.3 Hz), 8.17−8.04 (m, 5H, $H_{4,5,8,10,11}$), 7.88 (d, 1H, H_2, $J_{1,2}$ = 8.6 Hz); UV/vis (MeOH) λ_{max} (nm) (ϵ_{rel}) 212 (0.60), 234 (1.00), 312 (0.91), 389 (0.22), 410 (0.47), 433 (0.30), 461 (0.47); EI-MS *m/z* (rel intensity, %) 293 (24) $[MH]^+$, 292 (100) $[M]^+$, 263 (51) $[M - CHO]^+$.

Preparation of Subcellular Fractions. Adult male Sprague−Dawley rats (200−240 g; Interfauna Sueddeutsche Versuchstierfarm, Tuttlingen, Germany) were treated ip either with Aroclor 1254 (500 mg/kg body weight at day 6 before sacrifice), with 3-methylcholanthrene (40 mg/kg body weight at days 3, 2, and 1 before sacrifice), or with sodium phenobarbital (80 mg/kg body weight at days 3, 2, and 1 before sacrifice), or left untreated. Aroclor 1254 and 3-methylcholanthrene were dissolved in trioctanoin (2.5 mL/kg body weight), sodium phenobarbital in aqueous NaCl (0.9%; 2.5 mL/kg body weight). The postmitochondrial fraction, i.e., the 9000*g* supernatant, as well as the microsomal fraction of the liver was prepared as previously described (*25*) under sterile conditions. Protein concentrations were determined by the method of Lowry et al. (*26*) using bovine serum albumin for calibration. The P450 content was measured according to the procedure of Omura and Sato (*27*).

Metabolism Studies. Microsomal incubations contained liver microsomes equivalent to 4−5 nmol of P450, 0.6 mM $NADP^+$, 8 mM glucose 6-phosphate, 1.5 units of glucose-6-phosphate dehydrogenase, and 5 mM $MgCl_2$ in a final volume of 2 mL of 50 mM isotonic (150 mM KCl) sodium phosphate buffer (pH 7.4). In some cases, the incubation mixture contained 1 mM TCPO in 10 μL of acetone. This mixture was preincubated for 5 min at 37 °C. The incubation was started by the addition of 80 μM unlabeled or tritium-labeled anthanthrene (0.8−9.1 GBq [22−246 mCi]/mmol), 3-hydroxyanthanthrene (80 μM), or anthanthrene 4,5-oxide (25 μM) in 50 μL of Me_2SO and continued with shaking (80 min^{-1}) at 37 °C. The incubation was stopped with 2 mL of ice-cold ethyl acetate. After being vortexed for 1 min, the organic and aqueous phases were separated by centrifugation at 1500*g* and 20 °C for 5 min. The extraction was repeated twice more with 2 mL of ethyl acetate. The organic phases were combined, dried over anhydrous magnesium sulfate, and brought to dryness at 30−35 °C with a stream of nitrogen; then, the residue was stored at −70 °C until HPLC separation was performed, for which the sample was dissolved in 30 μL of Me_2SO.

All steps were performed under subdued light. The recovered radioactivity in the organic and aqueous phase was usually >95% of that applied.

Isolation of Acetylated Metabolites of Anthanthrene. Anthanthrene (90 μM) was incubated (80 min) as above in a final volume of 10 mL containing liver microsomes equivalent to 29 nmol of P450 of rats pretreated with Aroclor 1254. The incubation was stopped with 10 mL of ice-cold acetone and extracted with dichloromethane (25 mL). The organic phase was dried over anhydrous magnesium sulfate, concentrated to a volume of 100 μL, treated with 1.5 mL of a mixture of acetic anhydride/pyridine (1:2, v/v) for 16 h at room temperature, and subsequently brought to dryness with a stream of nitrogen. The residue was dissolved in Me_2SO and separated by HPLC [stationary phase: LiChrospher 100 RP-18, 5 μm, 250 × 4 mm; mobile phase: linear gradient of MeOH/H_2O (60:40, v/v) to 100% MeOH in 40 min; flow rate: 0.8 mL/min; detection wavelength: 254 nm]. Prominent peaks were collected and further purified by TLC on silica gel (60 F_{254}; Riedel-de-Haën, Seelze, Germany) with chloroform as the mobile phase. Bands visible under UV light were scraped off, eluted with acetone and dichloromethane (5 × 200 μL, each), and subjected to mass spectrometry (see below).

HPLC Analysis of Anthanthrene Metabolites. Chromatographic separations were performed with a system consisting of a ternary high-pressure pump (SP 8700; Spectra-Physics, Darmstadt, Germany), a sample injection valve (C6W; Valco, Schenkon, Switzerland) with a 25 μL sample loop, and a diode array detector (1100 series; Agilent Technologies, Karlsruhe, Germany) operated with LC 3D ChemStation A.08.03 software (Agilent Technologies) connected in line with a radioactivity flow-through detector (Ramona-LS, Raytest, Straubenhardt, Germany) operated with Chromasoft 0.3 software (Raytest).

For the chromatographic separation, 20 μL of the solution of the metabolites in Me_2SO was injected onto a Vertex column (4 × 250 mm; Knauer, Berlin) filled with LiChrospher 100 RP-18 (5 μm; Merck, Darmstadt, Germany) as the stationary phase. The mobile phase—kept at 1.5 bar under an atmosphere of helium—consisted of a mixture of MeOH and 10 mM aqueous NH_4HCO_3 (pH 8.0), with a linear increase in MeOH content from 65 to 100% (v/v) in 50 min followed by 100% MeOH for 20 min (separation of the metabolites of anthanthrene and of the 4,5-oxide) or of a mixture of MeOH/H_2O with a linear increase in MeOH content from 60 to 100% (v/v) in 40 min (separation of the metabolites of 3-phenol) at a flow rate of 0.8 mL/min. Anthanthrene-1,6- and 3,6-quinone coeluted under these conditions but could be separated employing Spherisorb S 5 ODS 2 as stationary and MeOH/H_2O as mobile phase with the linear increase in MeOH content and the flow rate as above. For the detection of radioactivity, the eluate was mixed in the radioactivity detector with liquid scintillator (Quickszint Flow 302, Zinsser Analytik, Frankfurt, Germany) at a ratio of 1:3.

Quantificaton of Metabolic Conversion. Total metabolic conversion was calculated from the sum of the radioactivity eluting upon HPLC before and after anthanthrene and of the radioactivity remaining in the aqueous phase after ethyl acetate extraction divided by the specific activity, *S*, of the substrate. The amount of distinct metabolites, *m*, was determined from the radiochromatogram by the formula: $m = (\mathrm{ROI}\cdot A)/(100\cdot S)$, where ROI (region of interest) is the percentage of radioactivity in the peak of the metabolite as compared to the total radioactivity in the radiochromatogram and *A* is the total radioactivity in the organic phase.

Spectral Methods. UV/vis absorption spectra of the synthetic derivatives of anthanthrene were obtained on a Shimadzu MPS-2000 spectrophotometer. UV/vis spectra of metabolites and of synthetic reference compounds were recorded on-line during HPLC with the diode array detector (cell volume: 13 μL; path length: 10 mm; peak width: >0.2 min; slit: 2 nm). Electron ionization (EI) mass spectra were recorded with a Varian MAT CH 7A spectrometer at 70 eV. Proton NMR spectra were measured on a Bruker AM 400 spectrometer at 400 MHz. Chemical shifts (in ppm) are relative to tetramethylsilane. Deuterated solvents were used as indicated for each compound.

Mutagenicity Studies. The mutagenicity experiments were performed as described by Ames et al. (*28*) with minor modifications (*29*). The auxotrophic strains TA97, TA98, TA100, and TA104 of *S. typhimurium* were generously provided by Dr. B. N. Ames, Berkeley, CA. The source and preparation of the postmitochondrial liver fraction are described above. The specific mutagenicity (his^+-revertant colonies/nmol) was calculated as the slope of the linear part of the dose—response curve.

Results

Bacterial Mutagenicity of Anthanthrene. As in the case of benzo[*a*]pyrene and of other tumorigenic PAH, anthanthrene did not revert strains TA97, TA98, TA100, and TA104 of *S. typhimurium* to histidine prototrophy without additional metabolic activation (data not shown). However, in the presence of the hepatic postmitochondrial fraction of Sprague—Dawley rats treated with Aroclor 1254 and an NADPH-generating system, anthanthrene was converted to mutagens for strains TA97, TA98, TA100, and TA104 in the range of 18—40 his^+-revertant colonies/nmol (Figure 1). This mutagenic effect amounted to 44—84% of the values observed for benzo[*a*]pyrene under the same conditions (Figure 1).

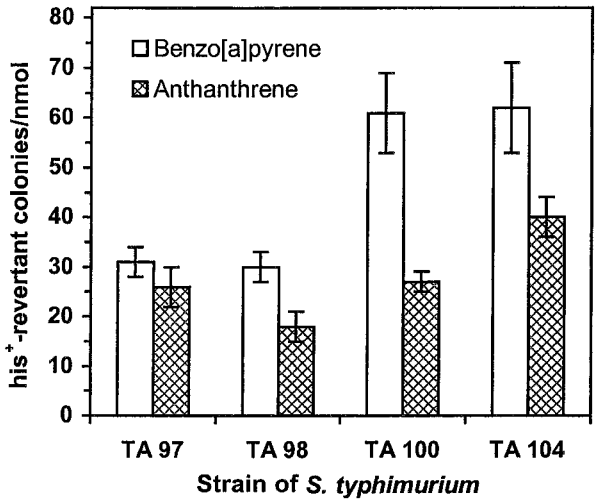

Figure 1. Bacterial mutagenicity in different strains of *S. typhimurium* of anthanthrene and benzo[*a*]pyrene metabolically activated with the postmitochondrial fraction of rats pretreated with Aroclor 1254. For details, see Experimental Procedures. Each bar represents the mean ± SD of three experiments.

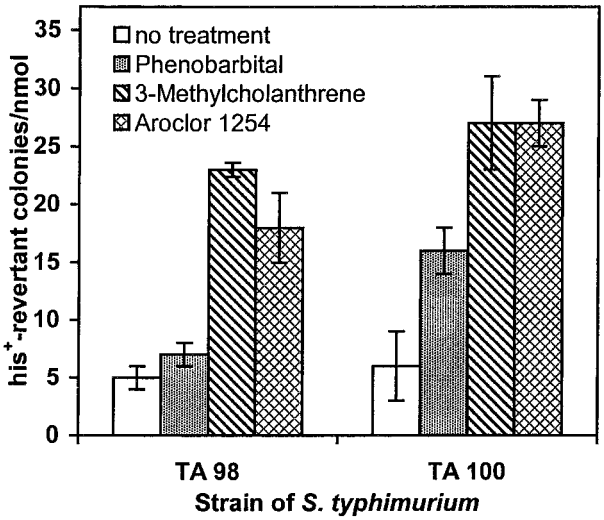

Figure 2. Bacterial mutagenicity in *S. typhimurium* TA98 and TA100 of anthanthrene metabolically activated with the postmitochondrial fraction of rats pretreated with different enzyme inducers. For details, see Experimental Procedures. Each bar represents the mean ± SD of three experiments.

The bacterial mutagenicity of anthanthrene is strongly dependent on the enzymatic composition of the postmitochondrial fraction as demonstrated with different enzyme inducers in strains TA98 and TA100 (Figure 2): The postmitochondrial fraction of untreated animals yielded just 5—6 his^+-revertant colonies/nmol; treatment of rats with phenobarbital led to an 1.4—2.7-fold increase in mutagenicity whereas treatment with 3-methylcholanthrene or Aroclor 1254, a mixture of polychlorinated biphenyls, raised the specific mutagenicity 3.6—4.6-fold to 18—27 his^+-revertant colonies/nmol.

Identification of Microsomal Metabolites of Anthanthrene. [G-^{3}H]Anthanthrene (80 μM) was incubated with liver microsomes of differently treated Sprague—Dawley rats equivalent to 2.5 nmol of P450/mL in the

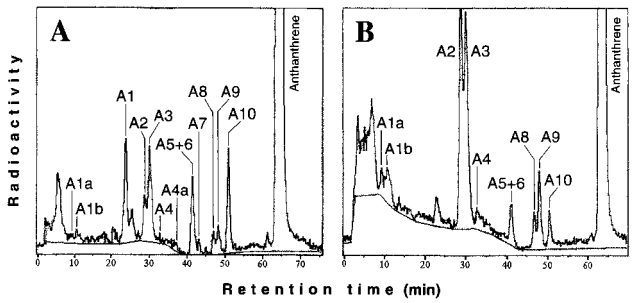

Figure 3. Radiochromatograms of the ethyl acetate-extractable metabolites of [G-^{3}H]anthanthrene incubated with liver microsomes of rats treated with phenobarbital (A) or 3-methylcholanthrene (B). For details, see Experimental Procedures. Roman numerals represent metabolites of anthanthrene (cf. Table 1).

presence of an NADPH-generating system for 20 min followed by ethyl acetate extraction of lipophilic metabolites. Reverse-phase HPLC separation of the extracts yielded the radiochromatograms of Figure 3A after phenobarbital and of Figure 3B after 3-methylcholanthrene treatment of the animals. In these chromatograms, 10 peaks, A1−A10, could be distinguished which were formed consistently, however in different amounts depending on the induction state. Metabolite A7 (Figure 3A) could only be detected when the aqueous portion of the mobile phase during HPLC separation consisted of NH_4HCO_3 solution (10 mM, pH 8) instead of pure water. Two peaks, A1a and A1b, eluting in the polar region of the chromatogram occurred somewhat erraticly often obscured by the radioactivity of tritiated water originating from [G-^{3}H]anthanthrene via formation of quinones. Similarly, metabolite A4a (Figure 3A) was not consistently formed.

The identification of most of the ethyl acetate-extractable metabolites of anthanthrene was achieved by a combination of (i) chromatographic, (ii) spectroscopic, and (iii) biochemical methods (Table 1). Metabolites A1, A7, A8, A9, and A10 (Figure 3A) coeluted with the 4,5-dihydrodiol, 4,5-oxide, 1-phenol, 3-phenol, and 6,12-quinone, respectively; the UV/vis spectra of the coeluting compounds were identical (Supporting Information: Figure S2, panels C, I, K, L, M). The metabolic formation of the 2-phenol, which is not well separated from the 3-phenol, could be excluded on the basis of different UV/vis spectra (Supporting Information: Figure S2, panel L). Metabolic conversion of synthetic 4,5-oxide with hepatic microsomes from phenobarbital-treated rats resulted in 10 peaks (E1−E10; Supporting Information: Figure S3) of which E2, E3, E5, and E6 coeluted with A1a, A1b, A1, and A4a (Table 1), exhibiting the same UV/vis spectra (Supporting Information: Figure S2, panels A, B, C, F). Due to their polarity and their origin from the 4,5-oxide, metabolites A1a and A1b probably contain more than two hydroxyl groups: in addition to the 4,5-dihydrodiol moiety, perhaps one or two phenolic hydroxyl groups. Metabolite A4a is very likely the 4,5-quinone since it has the same UV/vis spectrum as the synthetic compound (Supporting Information: Figure S2, panel F).

Metabolites A5 and A6 coeluted on LiChrospher 100 RP-18 (Figure 3) but could be well separated ($\alpha = 1.05$) by employing Spherisorb ODS 2 as the stationary phase. Under these conditions, coelution of A5 and A6 with the 1,6- and 3,6-quinone, respectively, as well as identity of their UV/vis spectra (Supporting Information: Figure S2, panels G, H) could be demonstrated. The ratio of metabolically formed 1,6-/3,6-quinone was determined to be 1:1.5.

An indication for the identity of A2 and A3, prominent metabolites in the case of microsomes of 3-methylcholanthrene-treated animals (Figure 3B), was obtained by comparison with the microsomal metabolites P1−P10 of the 3-phenol (Supporting Information: Figure S4). A2 and A3 coelute with P7 and P8, respectively (Table 1), and exhibit identical UV/vis spectra (Supporting Information: Figure S2, panels D, E). Thus, it is rather certain that A2 and A3 contain a hydroxyl group in the 3-position. With respect to their polarity, A2 and A3 could represent diphenols. This was further corroborated by acetylation of the isolated mixture of metabolites followed by HPLC as well as TLC separation as described under Experimental Procedures. The HPLC fraction at 33−35 min resulted in two bands with $R_f = 0.41$ and $R_f = 0.27$ upon TLC. The compound of the first band yielded the mass spectrum of Figure 4, which is typical for diacetoxyanthanthrene as depicted on the spectrum. The second band led to a mass spectrum with the molecular ion at $m/z = 306$ and sequential loss of two molecules of CO, leading to the fragment ions at $m/z = 278$ and $m/z = 250$ typical for quinones. Finally, an HPLC peak at 43.4 min exhibited a mass spectrum with the molecular ion at $m/z = 334$, loss of ketene leading to $m/z = 292$, and further loss of the fragment CHO to $m/z = 263$, a fragmentation pattern characteristical for a phenol acetate. Thus, the existence of quinones as well as phenols as metabolites of anthanthrene was additionally confirmed by this mass spectroscopic investigation.

Since A1a is metabolically formed from the 4,5-oxide (metabolite E2) as well as from the 3-phenol (metabolite P3; cf. Table 1), its identity with 4,5,9-trihydroxy-4,5-dihydroanthanthrene is almost certain. An additional indication that metabolites A1a, A1b, and A1 are dihydrodiols whereas metabolite A7 is an epoxide stems from their metabolic behavior in the presence of TCPO (1 mM), a potent inhibitor of microsomal epoxide hydrolase (*30*): The formation of A1a, A1b, and A1 is considerably depressed, in contrast to A7, the amount of which more than doubles, while the remaining metabolites are only marginally affected (Table 1).

Neither chromatographic nor UV/vis spectroscopic evidence for the microsomal formation of 6-methyl- or 6-hydroxymethylanthanthrene could be found under the metabolic conditions employed.

Influence of Enzyme Inducers on the Metabolic Conversion of Anthanthrene. A remarkable influence of the induction state of the metabolizing system on the bacterial mutagenicity of anthanthrene is demonstrated in Figure 2. The significance of enzyme induction is also reflected by the qualitatively as well as quantitatively different formation of microsomal metabolites (Figure 3). Hence, a quantitative assessment of the metabolic conversion of anthanthrene by hepatic microsomes of untreated rats and of rats treated with phenobarbital, 3-methylcholanthrene, and Aroclor 1254 was undertaken (Table 2). Of the amount of 160 nmol of anthanthrene applied, only 5.7% was metabolically converted in 20 min by microsomes of untreated rats containing 4 nmol of P450. Petreatment of the animals with phenobarbital raised the metabolic conversion 1.5-fold, while it is more than doubled in the case of 3-methylcholanthrene as well as Aroclor 1254 as compared to the untreated control.

Table 1. Criteria of Identity between Microsomal Metabolites of Anthanthrene, 3-Hydroxyanthanthrene, Anthanthrene 4,5-Oxide, and of Synthetic Derivatives of Anthanthrene

microsomal metabolites of						
anthanthrene[a,c] no.	3-hydroxy-anthanthrene[a,c,e] no.	anthanthrene 4,5-oxide[b,d,e] no.	synthetic derivatives of anthanthrene	corrected retention time[f] (min)	identity of UV spectra[g]	change in presence of TCPO[d,h] (%)
A1a	P3	E2		10.5	yes	16
A1b		E3		11.6	yes	8
A1		E5	*trans*-4,5-dihydrodiol	24.1	yes	4
A2	P7			29.2	yes	112
A3	P8			30.3	yes	69
A4				32.9		
A4a		E6	4,5-quinone	37.9	yes	
			6-hydroxymethyl	39.7		
A5			1,6-quinone	41.5	yes	126
A6	P10		3,6-quinone	41.6	yes	110
A7		substrate	4,5-oxide	43.4	yes	250
A8			1-phenol	47.2	yes	71
A9	substrate		3-phenol	48.4	yes	102
			2-phenol	48.5		
A10			6,12-quinone	51.2	yes	92
substrate			anthanthrene	64.7		
			6-methyl	69.8		

[a] 80 μM substrate concentration. [b] 25 μM substrate concentration. [c] Pretreatment of rats for the preparation of microsomes with Aroclor 1254 (see Table 2). [d] Pretreatment of rats for the preparation of microsomes with phenobarbital (see Table 2). [e] Only metabolites were tabulated that coelute with metabolites or synthetic derivatives of anthanthrene. [f] The retention time of different chromatographic runs was linearly adjusted using the retention time of common metabolites; for details on chromatographic conditions, see Experimental Procedures. [g] Supporting Information: Figure S2. [h] Change in the formation of metabolites of anthanthrene (80 μM) incubated in the presence or absence of 1,1,1-trichloro-2-propene oxide (TCPO; 1 mM); mean of two experiments. For details on incubation conditions, see Experimental Procedures.

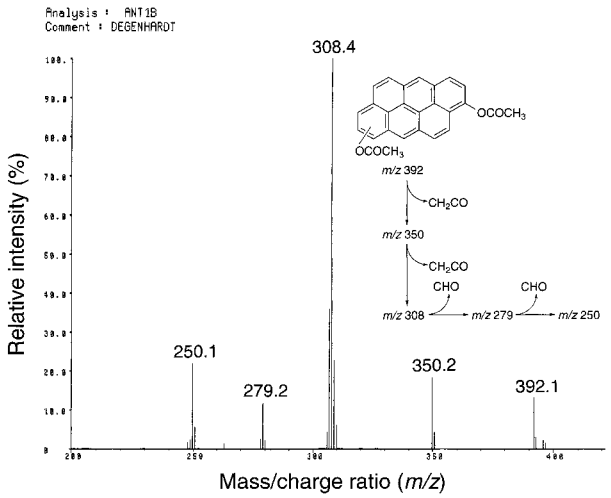

Figure 4. EI mass spectrum of an acetylated diphenolic metabolite of anthanthrene. For details, see Experimental Procedures.

Under this condition, the amount of metabolites extracted by ethyl acetate equaled that of free and protein-bound metabolites remaining in the aqueous phase due to their hydrophilicity. The portion of lipophilic metabolites after induction with phenobarbital and 3-methylcholanthrene was similarly raised to about 70% and declined in the case of Aroclor 1254 to about 60%. Large qualitative as well as quantitative differences in the formation of individual metabolites were observed when different inducers had been applied. Microsomes of untreated animals converted anthanthrene mainly to quinones and to polar as yet unidentified metabolites. The metabolites of anthanthrene formed with microsomes of phenobarbital-treated animals, on the other hand, were dominated by the 4,5-dihydrodiol (14.4% of the total metabolic conversion) followed by diphenol A3 (12.5%). Only under this condition was it possible to detect the K-region epoxide in a small amount (1.5%). About one-fifth of the total metabolic conversion consisted of polar metabolites. This amount declined in the case of microsomes of 3-methylcholanthrene-treated rats to 8%, whereas the metabolites were dominated by the diphenols A2 and A3, which summed up to 34.7% of total metabolic conversion. The K-region metabolites could not be detected. Of these, the 4,5-dihydrodiol was formed in a low amount (0.8%) when microsomes after treatment with Aroclor 1254 were employed. Again, the diphenols A2 and A3 were the principal metabolites with 29.4% of the total metabolic conversion.

Bacterial Mutagenicity of Metabolites of Anthanthrene and Its Influence by Enzyme Modulation. As mentioned above, anthanthrene did not exhibit bacterial mutagenicity without metabolic activation by rat liver enzymes. This was also the case with the 4,5-dihydrodiol and the 4,5-, 1,6-, 3,6-, and 6,12-quinones formed as microsomal metabolites of anthanthrene and available as synthetic compounds for determination of their mutagenicity in strain TA100 of *S. typhimurium* (Figure 5). In contrast, the K-region oxide as well as the 3-phenol are directly acting strong bacterial mutagens, whereas the 1-phenol is only weakly mutagenic without metabolic activation (Figure 5). The specific mutagenicity of the 3-phenol calculated as the slope of the linear part of the dose−response curve was 120 his^+-revertant colonies/nmol. In the case of the 4,5-oxide, a similar calculation was not possible due to lack of linearity of the dose−response curve. Therefore, an average slope of 279 his^+-revertant colonies/nmol in the dose range of 0.1−3.5 nmol/plate was determined for the K-region oxide of anthanthrene. The bacterial mutagenicity of the 4,5-oxide as well as the 3-phenol dropped considerably in the presence of the postmitochondrial fraction of Sprague−Dawley rats treated with Aroclor 1254 whereas the remaining derivatives of anthanthrene required enzymatic activation to exert mutagenicity (Figure 5). The strongest bacterial mutagens were formed from the 1-phenol with 38 his^+-revertant colonies/nmol; the mutagenicity of the 4,5-dihydrodiol amounted to 14 his^+-

Table 2. Metabolic Conversion of Anthanthrene (80 μM) by Liver Microsomes of Rats Treated with Different Enzyme Inducers

		metabolite formation [nmol (4 nmol of P450)$^{-1}$ (20 min)$^{-1}$] (% of total metabolic conversion) with enzyme inducer			
metabolites	no.[a]	(no treatment)	phenobarbital	3-methylcholanthrene	Aroclor 1254
polar metabolites[b]		1.59 ± 0.79 (17.5)	2.86 ± 0.39 (20.8)	1.58 ± 1.09 (8.0)	2.71 ± 0.77 (13.3)
trans-4,5-dihydrodiol	A1	0.08 ± 0.02 (0.9)	1.98 ± 0.89 (14.4)	<0.01	0.17 ± 0.10 (0.8)
3,?-diphenol	A2	0.23 ± 0.14 (2.5)	0.77 ± 0.24 (5.6)	4.06 ± 1.93 (20.5)	3.15 ± 2.32 (15.5)
3,?-diphenol	A3	0.12 ± 0.08 (1.3)	1.72 ± 0.47 (12.5)	2.80 ± 1.42 (14.2)	2.83 ± 1.68 (13.9)
	A4	0.07 ± 0.13 (0.8)	0.12 ± 0.05 (0.9)	2.68 ± 2.08 (13.6)	0.27 ± 0.13 (1.3)
1,6- + 3,6-quinone	A5+A6	0.77 ± 0.30 (8.5)	0.87 ± 0.25 (6.3)	1.34 ± 0.90 (6.8)	0.94 ± 0.31 (4.6)
4,5-oxide	A7	<0.01	0.21 ± 0.06 (1.5)	<0.01	<0.01
1-phenol	A8	≈0.01 (0.1)	0.24 ± 0.14 (1.7)	0.04 ± 0.10 (0.2)	0.06 ± 0.13 (0.3)
3-phenol	A9	0.02 ± 0.01 (0.2)	0.37 ± 0.20 (2.7)	0.20 ± 0.22 (1.0)	0.17 ± 0.28 (0.8)
6,12-quinone	A10	1.03 ± 0.26 (11.3)	0.47 ± 0.32 (3.4)	—[c]	—[c]
unknown ethyl acetate-extractable metabolites[d]		0.56 ± 0.47 (6.1)	0.62 ± 0.47 (4.5)	0.71 ± 1.31 (3.6)	1.46 ± 1.87 (7.2)
total ethyl acetate-extractable metabolites		4.48 ± 0.99 (49)	10.23 ± 2.79 (74)	13.41 ± 4.26 (68)	11.76 ± 3.62 (58)
water-soluble and protein-bound metabolites		4.63 ± 2.59 (51)	3.53 ± 0.84 (26)	6.35 ± 3.66 (32)	8.57 ± 3.23 (42)
total metabolic conversion		9.11 ± 3.21 (100)	13.76 ± 3.34 (100)	19.76 ± 5.79 (100)	20.33 ± 6.48 (100)

[a] See Table 1. [b] Metabolites eluting before anthanthrene 4,5-dihydrodiol (A1). [c] Amount often lower than in incubations without microsomal protein. [d] Calculated from the total radioactivity of the chromatographic run after subtraction of the background, of the radioactivity of the substrate, and of the distinct metabolic peaks (A1−A10) including the polar metabolites; values represent means ± SD of 3−6 incubations.

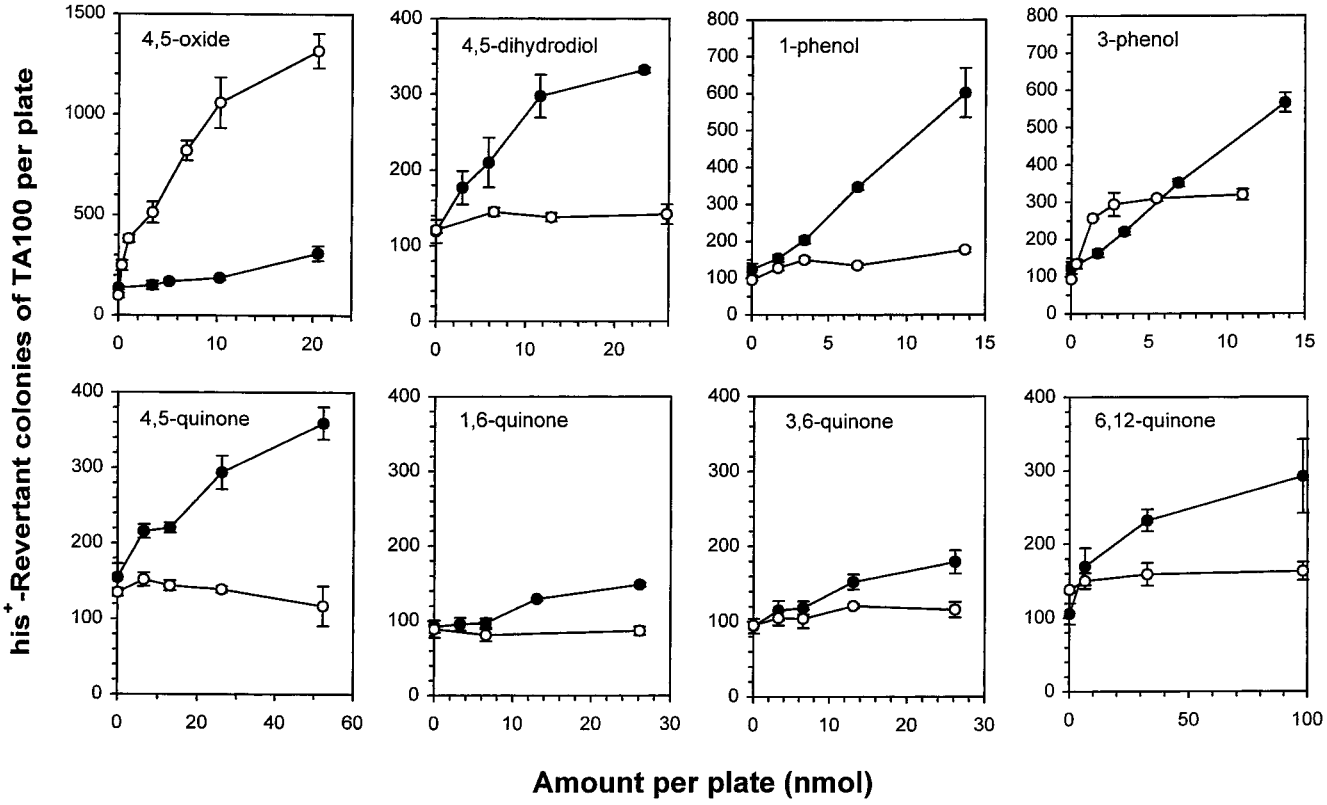

Figure 5. Bacterial mutagenicity in *S. typhimurium* TA100 of metabolically relevant synthetic derivatives of anthanthrene in the presence (solid symbols) or absence (open symbols) of the postmitochondrial fraction of rats pretreated with Aroclor 1254. For details, see Experimental Procedures. Each point represents the mean ± SD of three experiments.

revertant colonies/nmol, while only weakly mutagenic metabolites were formed from the K-region quinone as well as from the three polynuclear quinones (3−5 his$^+$-revertant colonies/nmol).

The inhibition of xenobiotic metabolizing enzymes in the Ames test allows an estimation of the significance of these enzymes in the activation of the test compound or its metabolites to mutagenic intermediates. 7,8-Benzoflavone, an inhibitor of the P450 1A subfamily (*31*), lowered in a concentration of 50 μM in the top agar the mutagenicity of anthanthrene to one-third in strains TA98 and TA100 (Table 3). The bacterial mutagenicity of the 3-phenol and the 4,5-oxide was also depressed in the presence of 7,8-benzoflavone, however, only to 60−70%, while that of the 4,5-dihydrodiol dropped to an average of 23%.

Inhibition of the epoxide hydrolase by TCPO could only be investigated in strain TA98 since this epoxide is mutagenic in strain TA100. When the top agar contained 1 mM TCPO, the mutagenicity of anthanthrene and of

Table 3. Influence of Inhibitors of Phase I and Cofactors of Phase II Enzymes on the Bacterial Mutagenicity of Anthanthrene and Some of Its Metabolically Relevant Derivatives[a]

compound	bacterial strain	specific mutagenicity[b] (his$^+$-rev./nmol)	change (%) of specific mutagenicity in the presence of				
			7,8-benzoflavone[c]	TCPO[d]	GSH[e]	UDPGA + UDPAG[f]	ATP + sulfate[g]
anthanthrene	TA98	18 ± 3 (7 ± 1)[h]	33/45	139 ± 3 (286 ± 16)[h]	77/72	27/45	94 ± 6
	TA100	27 ± 2	33 ± 6	nd	70 ± 22	55 ± 22	103 ± 15
3-hydroxyanthanthrene	TA98	15 ± 5	nd[i]	112/202	nd	nd	nd
	TA100	31 ± 6	53/64	nd	55 ± 10	16/29	97/74
anthanthrene 4,5-oxide	TA98	5/5 (7 ± 4)[h]	nd	220/224 (974/604)[h]	nd	nd	nd
	TA100	13/8	54/88	nd	46/87	31/25	77/137
anthanthrene 4,5-dihydrodiol	TA98	5 ± 1 (4 ± 1)[h]	44/72	178/210 (140/173)[h]	nd	nd	nd
	TA100	9 ± 2	16/30	nd	33/22	33/33	144/67

[a] Values are means ± SD of at least three experiments or individual results of two experiments. [b] Metabolizing system: hepatic postmitochondrial fraction of rats pretreated with Aroclor 1254. [c] 50 μM. [d] 1,1,1-Trichloro-2-propene oxide (TCPO; 1 mM). [e] 5 mM. [f] Uridine 5′-diphosphoglucuronic acid (UDPGA; 4 mM) and uridine 5′-diphospho-*N*-acetylglucosamine (UDPAG; 4 mM). [g] ATP (10 mM) and sodium sulfate (5 mM); all concentrations are related to the top agar mixture. [h] Metabolizing system: hepatic postmitochondrial fraction of rats pretreated with phenobarbital. [i] nd = not determined.

its 3-phenol increased by about 40−60% while the mutagenic effect of the K-region epoxide and the dihydrodiol was doubled (Table 3). Treatment of the animals used for the preparation of the hepatic postmitochondrial fraction with phenobarbital instead of Aroclor 1254 led to an even more pronounced effect of TCPO: The mutagenicity of anthanthrene was raised nearly 3-fold and that of the K-region epoxide up to 10-fold (Table 3).

In the standard Ames test, phase II enzymes are usually not operative since due to dilution of the postmitochondrial fraction the concentration of their cofactors falls considerably below the K_m values. Hence, the influence of conjugating enzymes on the bacterial mutagenicity of a compound can be studied by adding the necessary cofactor to the top agar. In the presence of 5 mM GSH, the mutagenic effect of anthanthrene and of its 4,5-oxide was reduced to about 70%. The mutagenicity of the 3-phenol dropped under this condition to 55% while the strongest influence of the GSH transferase with an average reduction to 28% was observed in the case of the 4,5-dihydrodiol (Table 3). The UDP-glucuronosyltransferase depressed the bacterial mutagenicity of anthanthrene and of its metabolically relevant derivatives more efficiently than both other phase II enzymes investigated (Table 3). Addition of 4 mM UDPGA and of 4 mM UDPAG as activator of UDP-glucuronosyltransferase (*32*) to the top agar lowered the mutagenicity in all cases down to one-third. The sulfotransferase, in contrast, put into action by the PAPS generating system ATP/sulfate, exhibited with 86% only a weak reducing effect in the case of the 3-phenol while the mutagenicity of the remaining compounds including anthanthrene remained virtually unchanged (Table 3).

Discussion

Although anthanthrene lacks a bay-region and hence the requirement for formation of bay-region dihydrodiol epoxides thought to be responsible for the genotoxicity of PAH, it nevertheless exhibits remarkably strong bacterial mutagenicity after metabolic activation comparable with that of benzo[*a*]pyrene (*33*). Based on the sensitivity of the strains of *S. typhimurium* used, the metabolites of anthanthrene are able to cause base-pair substitutions (TA100), frameshifts (TA98, TA97), and possibly oxidative damage (TA104) in the bacterial DNA. As in the case of other PAH, the enzymatic composition of the metabolizing system determines the extent of mutagenicity of anthanthrene. The enzymes of the P450 1A subfamily, induced by 3-methylcholanthrene, convert anthanthrenes like benzo[*a*]pyrene (*34, 35*) to the most potent mutagenic metabolites, but in contrast to benzo[*a*]pyrene (*34, 35*), the enzymes of the P450 2B subfamily, induced by phenobarbital, also play a role in the activation of anthanthrene to mutagens for strain TA100.

To elucidate the metabolites of anthanthrene responsible for its mutagenicity, the phase I biotransformation was investigated. By employing synthetic derivatives of anthanthrene and combining chromatographic, spectroscopic, and biochemical methods, 12 microsomal metabolites could be fully or at least partially identified. Among them, three metabolites at the K-region, the 4,5-oxide (A7), 4,5-dihydrodiol (A1), and 4,5-quinone (A4a), were found. As in the case of benzo[*a*]pyrene (*36*) and dibenz[*a,h*]anthracene (*37*), the isomerization of the K-region oxide of anthanthrene (A7) could only be prevented when its chromatographic separation was performed under slightly alkaline conditions. Furthermore, three polynuclear quinones, the 1,6- (A5), 3,6- (A6), and 6,12-positional (A10) isomers, as well as two phenols, the 1- (A8) and 3-positional (A9) isomers, could be detected. Two major metabolites derived from the 3-phenol turned out to be diphenols (A2, A3). This corresponds to results obtained with benzo[*a*]pyrene that pointed to the existence of the 3,6- (*38, 39*) and 3,9-diphenols (*38*). Hence, A2 and A3 are tentatively identified as 3,6- and 3,9-dihydroxyanthanthrene. One polar metabolite of anthanthrene could be the 3-phenol 4,5-dihydrodiol since it is formed not only from the 4,5-oxide but also from the 3-phenol. However, since the second monooxygenase attack occurs more likely distant and not vicinal to the first attack, this metabolite is instead the 9-phenol 4,5-dihydrodiol (A1a), the 9-position being identical with the 3-position due to the rotational symmetry of anthanthrene. Another polar metabolite is probably also a phenol dihydrodiol (A1b) arising from the 4,5-oxide. A homologous phenol oxide of benzo[*a*]pyrene, the 9-hydroxy 4,5-oxide, has been postulated as an ultimate mutagen of this PAH (*40*), alkylating the DNA possibly after rearrangement to a quinone-methide (*41*).

With the information on the structures of the microsomal metabolites of anthanthrene, the pattern of its biotransformation exhibiting three distinct pathways can be envisaged (Scheme 2). Pathway I starts with the epoxidation at the K-region leading to the 4,5-oxide, which is then hydrolyzed to the 4,5-dihydrodiol, the oxidation of which yields the K-region quinone in traces. Whether the two phenol dihydrodiols A1a and A1b are

Scheme 2. Pathways of Microsomal Biotransformation of Dibenzo[*def,mno*]chrysene (Anthanthrene)[a]

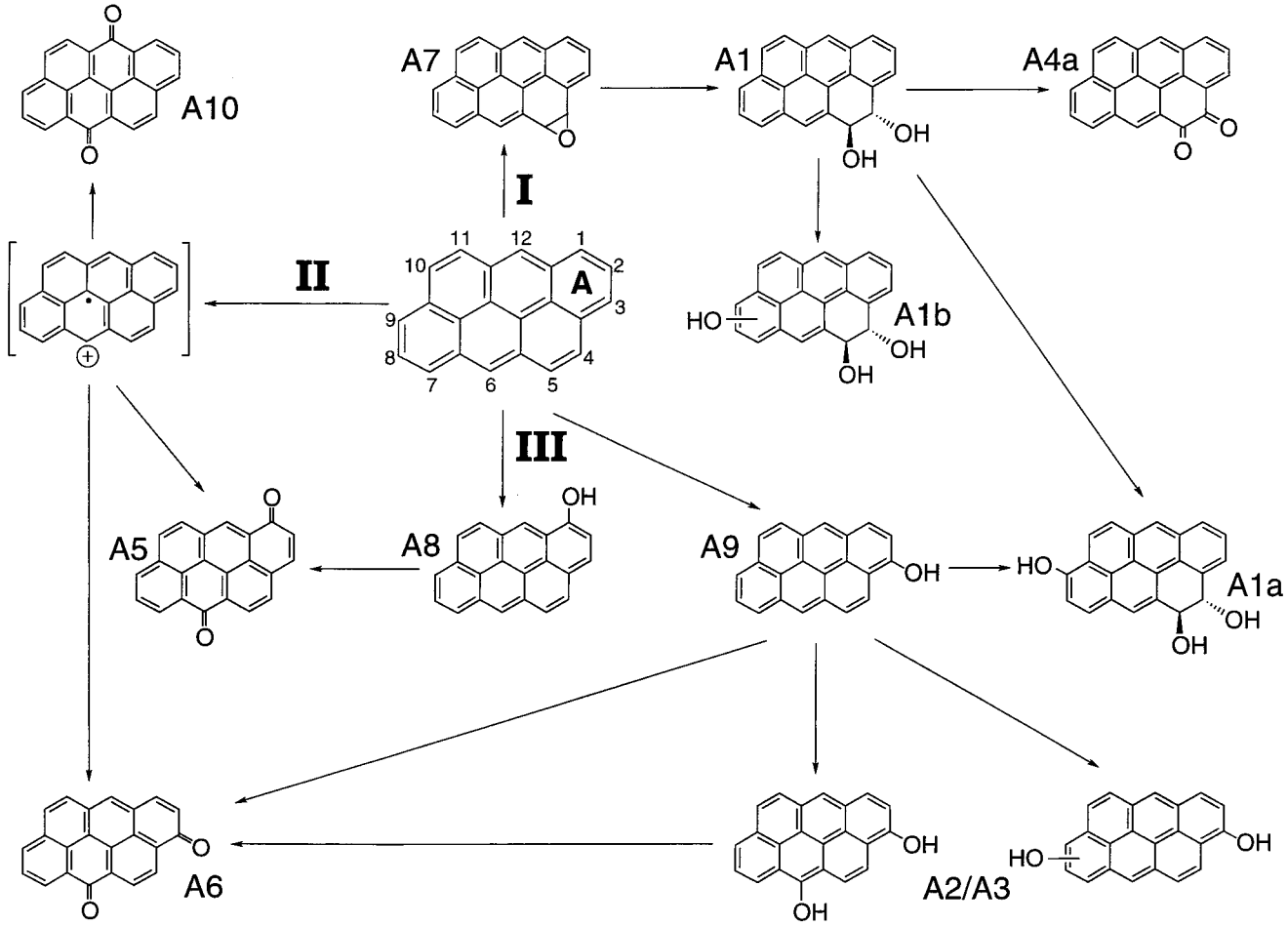

[a] In the case of chiral metabolites, only one arbitrary enantiomer is shown. For the meaning of the Roman numerals, see Table 1.

formed directly from the 4,5-oxide or via the 4,5-dihydrodiol as depicted in Scheme 2 cannot be decided at present. As observed with other PAH (*42*, *43*), monooxygenation of anthanthrene at the K-region is preferentially catalyzed by the P450 2B subfamily. The formation of metabolites A1, A1a, and A1b is considerably depressed by inhibition of epoxide hydrolase, proving the importance of this hydrolytic enzyme in pathway I.

The 6,12-quinone and possibly the other polynuclear quinones of anthanthrene can be formed via pathway II (Scheme 2) by one-electron oxidation as proposed for benzo[*a*]pyrene (*44*). However, due to the connection of pathways II and III, this statement is not unequivocal. In contrast to the other metabolites of anthanthrene, neither the inducible P450 1A nor 2B enzymes are considerably involved in the formation of the polynuclear quinones. Especially in the case of the 6,12-quinone, autoxidation of anthanthrene seems to be more relevant than its enzymatic conversion.

Pathway III starts with the monooxygenation at the A-ring of anthanthrene yielding the 1- and 3-phenols. Further oxidation of the latter is observed at the 6-position, at the 10,11-position (K-region), and at a third yet unknown position leading to 3,6-diphenol (A2 or A3), 3-phenol 10,11-dihydrodiol (A1a; after enzymatic hydrolysis), and another diphenol, possibly the 3,9-positional isomer (A2 or A3). Oxidation of the 1-phenol could produce the 1,6-quinone, while the 3,6-quinone is either formed directly from the 3-phenol or formed via the 3,6-diphenol. Enzymatic monooxygenation in this pathway is dominated by the P450 1A subfamily whereas P450 2B plays only a minor role.

With the information on the mutagenicity of the metabolites of anthanthrene, it is now possible to evaluate the contribution of the three metabolic pathways to the genotoxicity of the parent hydrocarbon. The quinones of anthanthrene constituting rather weak mutagens are preferentially formed under conditions where the hydrocarbon exhibits the lowest bacterial mutagenicity. These observations make it less likely that pathway II contributes much to the genotoxicity of anthanthrene. Among the identified metabolites of anthanthrene, there are only two which exhibit strong bacterial mutagenicity without metabolic activation: the 3-phenol and the 4,5-oxide. On a molar basis, their specific mutagenicity is about 4.4−10.3-fold higher than that of anthanthrene after metabolic activation. Thus, ultimate mutagens of anthanthrene are produced via pathway I as well as via pathway III.

The role of monooxygenases of the P450 2B subfamily in activation of anthanthrene to mutagenic metabolites and their inactivation by epoxide hydrolase in pathway I is reflected by a considerable increase of mutagenicity upon inhibition of epoxide hydrolase by TCPO, an effect that was especially strong when the metabolizing enzymes had been induced with phenobarbital. Likewise, the significance of monooxygenases of the P450 1A subfamily in transforming anthanthrene to mutagenic metabolites could be demonstrated by inhibition with 7,8-

Table 4. Significance of 3-Hydroxylation Compared to 4,5-Epoxidation for the Genotoxicity of Anthanthrene

Specific Mutagenicity[a]			
his$^+$-rev. colonies of TA100/nmol in			
3-hydroxyanthanthrene		anthanthrene 4,5-oxide	
120		279	
Metabolic Conversion			
nmol (nmol of P450)$^{-1}$ (20 min)$^{-1}$ in hepatic microsomes of rats after treatment with			
phenobarbital		3-methylcholanthrene	
3-hydroxylation[b]	4,5-epoxidation[c]	3-hydroxylation[b]	4,5-epoxidation[c]
0.85	0.55	1.97	<0.01
Calculated Maximal Number of *his*$^+$-rev. Colonies of TA100 (nmol of P450)$^{-1}$(20 min)$^{-1}$			
102	153	236	<3

[a] Spontaneous mutagenicity. [b] Sum of 3-phenol, diphenols A2 and A3, as well as 3,6-quinone (=60% of the mixture 1,6-/3,6-quinone). [c] Sum of 4,5-oxide and *trans*-4,5-dihydrodiol.

benzoflavone. Finally, the remarkable reduction of the mutagenicity of anthanthrene and of its 3-phenol by UDG-glucuronosyltransferase is an indication for the formation of phenolic metabolites on the route to ultimate mutagens.

For the evaluation of the significance of pathways I and III for the genotoxicity of anthanthrene, not only the intrinsic mutagenicity of the 4,5-oxide and that of the 3-phenol but also the total metabolic formation of these two metabolites including their secondary metabolites has to be taken into account. Calculating the maximal mutagenic effect from these two parameters (Table 4) demonstrates the dominating role of the 3-hydroxylation pathway III in the mutagenicity of anthanthrene under conditions where this hydrocarbon exhibits the strongest bacterial mutagenicity, that is, after induction with 3-methylcholanthrene.

Since the 3-phenol is mutagenic without enzymatic activation, the formation of a phenol epoxide as an ultimately mutagenic metabolite (*40*, *41*) can be excluded. Recently we could demonstrate the spontaneous conversion of the 3-phenol to fairly stable phenoxy radicals by ESR measurements (*45*). These radical species could be responsible for the genotoxicity of anthanthrene similarly as it has been assumed for the 6-oxobenzo[*a*]pyrene radical (*46*). The spontaneous formation of phenoxy radicals from 3-hydroxyanthanthrene seems to be rather unique for this PAH since 3-hydroxybenzo[*a*]pyrene could not be converted to radical species under the same conditions (*45*). Therefore, although 3-hydroxybenzo[*a*]-pyrene is the most prominent microsomal metabolite of this PAH in the presence of P450 1A (*47*), it rather constitutes an inactivation step by virtue of its conjugation (*48*, *49*) whereas in the case of anthanthrene its 3-phenol is the precursor of an ultimate mutagen.

Anthanthrene has one of the lowest ionization potentials of all PAH (*2*) and could therefore undergo one-electron oxidation to radical cations preferentially at the L-region (6,12-position in anthanthrene; cf. Scheme 1). These electrophilically reactive species could covalently bind to DNA and as a consequence cause genotoxicity (*2*). The occurrence of polynuclear quinones in the biotransformation of PAH is thought to be an indication for the initial formation of radical cations (*44*). However, since the amount of polynuclear quinones of anthanthrene is highest under conditions where this PAH exhibits the lowest mutagenic effect, an appreciable contribution of one-electron oxidation to the genotoxicity of anthanthrene is not very likely. The L-region of anthanthrene could also be the location for enzymatic methylation or hydroxymethylation as described for other PAH with a *meso*-anthracenic center (*3*). The resulting benzylic alcohols can be substrates of sulfotransferase(s), transforming them to highly reactive esters. Remarkably, the conversion of 6-hydroxymethylanthanthrene to strong bacterial mutagens by sulfotransferases of the rat has already been demonstrated (*50*). However, no indication for the metabolic formation of 6-methyl- or 6-hydroxymethylanthanthrene could be found under the metabolic conditions employed in this study. This result excludes the "bioalkylation" as playing a role in the genotoxicity of anthanthrene. Eventually, hitherto unknown metabolites of anthanthrene could have escaped detection by reaction with nucleophilic sites in proteins. Thus, investigations on the binding of metabolites of anthanthrene to biomolecules such as proteins or DNA and identification of the covalent adducts could shed more light on the enzymatic activation of this mutagenic PAH without a bay-region to genotoxic metabolites.

Acknowledgment. We express our appreciation to M. Tommasone and B. Beile for excellent technical assistance. The help of M. Eider and A. Vierengel in performing the mass and NMR spectra is gratefully acknowledged. We thank the Deutsche Forschungsgemeinschaft for financial support (Grants SFB 302 and PL 115/1-1).

Supporting Information Available: Scheme S1 showing the synthesis of the non-K-region phenols of anthanthrene, Figure S2 depicting UV/vis spectra of metabolites of anthanthrene, 3-hydroxyanthanthrene, anthanthrene 4,5-oxide, and of synthetic derivatives of anthanthrene recorded during HPLC separation with the diode array detector, and also Figures S3 and S4 exhibiting HPLC separations of the metabolites of the 4,5-oxide (E1−E10) and of the 3-phenol (P1−P10), respectively. This material is available free of charge via the Internet at http://pubs.acs.org.

References

(1) Jerina, D. M., Sayer, J. M., Agarwal, S. K., Yagi, H., Levin, W., Wood, A. W., Conney, A. H., Pruess-Schwartz, D., Baird, W. M., Pigott, M. A., and Dipple, A. (1986) Reactivity and tumorigenicity of bay-region diol epoxides derived from polycyclic aromatic hydrocarbons. In *Biological Reactive Intermediates III. Mechanisms of Action in Animal Models and Human Disease* (Kocsis, J. J., Jollow, D. J., Witmer, C. M., Nelson, J. O., and Snyder, R., Eds.) pp 11−30, Plenum Press, New York and London.

(2) Cavalieri, E. L., and Rogan, E. G. (1995) Central role of radical cations in metabolic activation of polycyclic aromatic hydrocarbons. *Xenobiotica* **25**, 677−688.

(3) Flesher, J. W., and Myers, S. R. (1990) Bioalkylation of benz[*a*]-anthracene as a biochemical probe for carcinogenic activity. Lack of bioalkylation in a series of six noncarcinogenic polynuclear aromatic hydrocarbons. *Drug Metab. Dispos.* **18**, 163−167.

(4) Shou, M., Harvey, R. G., and Penning, T. M. (1993) Reactivity of benzo[*a*]pyren-7,8-dione with DNA. Evidence for the formation of deoxyguanosine adducts. *Carcinogenesis* **14**, 475−482.

(5) Yang, Y., Griffiths, W. J., Nordling, M., Nygren, J., Möller, L., Bergman, J., Liepinsh, E., Otting, G., Gustafsson, J.-A., Rafter, J., and Sjövall, J. (2000) Ring opening of benzo[*a*]pyrene in the germ-free rat is a novel pathway for formation of potentially genotoxic metabolites. *Biochemistry* **39**, 15585−15591.

(6) Stansbury, K. H., Noll, D. M., Groopman, J. D., and Trush, M. A. (2000) Enzyme-mediated dialdehyde formation: An alternative pathway for benzo[*a*]pyrene 7,8-dihydrodiol bioactivation. *Chem. Res. Toxicol.* **13**, 1174−1180.

(7) IARC Working Group (1983) Anthanthrene. In *IARC Monographs on the Evaluation of the Carcinogenic Risk of Chemicals to Humans. Polynuclear Aromatic Compounds, Part 1, Chemical,*

Environmental and Experimental Data, Vol. 32, pp 95−104, International Agency for Research on Cancer, Lyon, France.

(8) Andrews, A. W., Thibault, L. H., and Lijinski, W. (1978) The relationship between carcinogenicity and mutagenicity of some polynuclear hydrocarbons. *Mutat. Res.* **51**, 311−318.

(9) Kaden, D. A., Hites, R. A., and Thilly, W. G. (1979) Mutagenicity of soot and associated polycyclic aromatic hydrocarbons to *Salmonella typhimurium*. *Cancer Res.* **39**, 4152−4159.

(10) LaVoie, E., Bedenko, V., Hirota, N., Hecht, S. S., and Hoffmann, D. (1979) A comparison of the mutagenicity, tumor-initiating activity and complete carcinogenicity of polynuclear aromatic hydrocarbons. In *Polynuclear Aromatic Hydrocarbons* (Jones, P. W., and Leber, P., Eds.) pp 705−721, Ann Arbor Science Publishers, Ann Arbor, MI.

(11) Hermann, M. (1981) Synergistic effects of individual polycyclic aromatic hydrocarbons on the mutagenicity of their mixtures. *Mutat. Res.* **90**, 399−409.

(12) Cavalieri, E., Mailander, P., and Pelfrene, A. (1977) Carcinogenic activity of anthanthrene on mouse skin. *Z. Krebsforsch.* **89**, 113−118.

(13) Scribner, J. D. (1973) Tumor initiation by apparently noncarcinogenic polycyclic aromatic hydrocarbons. *J. Natl. Cancer Inst.* **50**, 1717−1719.

(14) Deutsch-Wenzel, R. P., Brune, H., Grimmer, G., Dettbarn, G., and Misfeld, J. (1983) Experimental studies in rat lungs on the carcinogenicity and dose−response relationships of eight frequently occurring environmental polycyclic aromatic hydrocarbons. *J. Natl. Cancer Inst.* **71**, 539−544.

(15) Clar, E. (1939) Die Zinkstaubschmelze. Eine neue Methode zur Reduktion organischer Verbindungen. *Ber. Dtsch. Chem. Ges.* **72**, 1645−1649.

(16) Jacob, J., Karcher, W., and Wagstaffe, P. J. (1984) Polycyclic aromatic compounds of environmental and occupational importance−Their occurrence, toxicity and the development of high purity certified reference materials, Part I. *Fresenius J. Anal. Chem.* **317**, 101−114.

(17) Cho, H., and Harvey, R. G. (1976) Synthesis of hydroquinone diacetates from polycyclic aromatic quinones. *J. Chem. Soc., Perkin Trans. 1*, 836−839.

(18) Lehr, R. E., Taylor, C. W., Kumar, S., Mah, H. D., and Jerina, D. M. (1978) Synthesis of the non-K-region and K-region *trans*-dihydrodiols of benzo[*e*]pyrene. *J. Org. Chem.* **43**, 3462−3466.

(19) Platt, K. L., and Oesch, F. (1982) K-region *trans*-dihydrodiols of polycyclic arenes; an efficient and convenient preparation from *o*-quinones or *o*-diphenols by reduction with sodium borohydride in the presence of oxygen. *Synthesis*, 459−462.

(20) Harvey, R. G., Goh, S. H., and Cortez, C. (1975) "K-Region" oxides and related oxidized metabolites of carcinogenic aromatic hydrocarbons. *J. Am. Chem. Soc.* **97**, 3468−3479.

(21) Buu-Hoi, N. P., and Lavit, D. (1957) Hydrocarbures polycycliques aromatiques. III. Dérivés de substitution de l'anthanthrène. *Recl. Trav. Chim. Pays-Bas* **76**, 200−205.

(22) Seidel, A., Bochnitschek, W., Glatt, H. R., Hodgson, R. M., Grover, P. L., and Oesch, F. (1991) Activated metabolites of chrysene: synthesis of 9-hydroxychrysene-1,2-diol and the corresponding bay-region *syn*- and *anti*-triol-epoxides. In *Polynuclear Aromatic Hydrocarbons: Measurements, Means and Metabolism* (Coole, M., Loening, K., and Meritt, J., Eds.) pp 801−817, Battelle Press, Columbus, OH.

(23) Luch, A., Glatt, H., Platt, K. L., Oesch, F., and Seidel, A. (1994) Synthesis and mutagenicity of the diastereomeric fjord-region 11,-12-dihydrodiol 13,14-epoxides of dibenzo[*a*,*l*]pyrene. *Carcinogenesis* **15**, 2507−2516.

(24) Seidel, A., Luch, A., Platt, K. L., Oesch, F., and Glatt, H. R. (1994) Activated fjord-region metabolites of dibenzo[*a*,*l*]pyrene: Synthesis and mutagenic activities of the diastereomeric *syn*- and *anti*-11,12-dihydrodiol 13,14-epoxides. *Polycyclic Aromatic Compd.* **6**, 191−198.

(25) Schmassmann, H., Sparrow, A., Platt, K., and Oesch, F. (1978) Epoxide hydratase and benzo[*a*]pyrene monooxygenase activities in liver, kidney and lung after treatment of rats with epoxides of widely varying structures. *Biochem. Pharmacol.* **27**, 2237−2245.

(26) Lowry, O. H., Rosebrough, N. J., Farr, A. L., and Randall, R. J. (1951) Protein measurement with the Folin phenol reagent. *J. Biol. Chem.* **193**, 265−275.

(27) Omura, T., and Sato, R. (1964) The carbon monoxide-binding pigment of liver microsomes. II. Solubilization, purification, and properties. *J. Biol. Chem.* **239**, 2379−2385.

(28) Ames, B. N., McCann, J., and Yamasaki, E. (1975) Methods for detecting carcinogens and mutagens with the *Salmonella*/mammalian-microsome mutagenicity test. *Mutat. Res.* **31**, 347−363.

(29) Platt, K. L., and Schollmeier, M. (1994) Bisdihydrodiols, rather than dihydrodiol oxides, are the principal microsomal metabolites of tumorigenic *trans*-3,4-dihydroxy-3,4-dihydrodibenz[*a*,*h*]anthracene. *Chem. Res. Toxicol.* **7**, 89−97.

(30) Oesch, F., Kaubisch, N., Jerina, D. M., and Daly, J. W. (1971) Hepatic epoxide hydrase. Structure−activity relationships for substrates and inhibitors. *Biochemistry* **10**, 4858−4866.

(31) Halpert, J. R., Guengerich, F. P., Bend, J. R., and Correia, M. A. (1994) Selective inhibitors of cytochromes P450. *Toxicol. Appl. Pharmacol.* **125**, 163−175.

(32) Vessey, D. A., Goldenberg, J., and Zakim, D. (1973) Kinetic properties of microsomal UDP-glucuronyltransferase. Evidence for cooperative kinetics and activation by UDP-*N*-acetylglucosamine. *Biochim. Biophys. Acta* **309**, 58−66.

(33) McCann, J., Spingarn, N. E., and Kobori, B. N. (1975) Detection of carcinogens as mutagens: Bacterial tester strains with R factor plasmids. *Proc. Natl. Acad. Sci. U.S.A.* **72**, 979−983.

(34) Wood, A. W., Levin, W., Lu, A. Y. H., Yagi, H., Hernandez, O., Jerina, D. M., and Conney, A. H. (1976) Metabolism of benzo[*a*]-pyrene and benzo[*a*]pyrene derivatives to mutagenic products by highly purified hepatic microsomal enzymes. *J. Biol. Chem.* **251**, 4882−4890.

(35) Bentley, P., Oesch, F., and Glatt, H. (1977) Dual role of epoxide hydratase in both activation and inactivation of benzo[*a*]pyrene. *Arch. Toxicol.* **39**, 65−75.

(36) Selkirk, J. K., Croy, R. G., and Gelboin, H. V. (1975) Isolation by high-pressure liquid chromatography and characterization of benzo[*a*]pyrene-4,5-epoxide as a metabolite of benzo[*a*]pyrene. *Arch. Biochem. Biophys.* **168**, 322−326.

(37) Platt, K. L., and Reischmann, I. (1987) Regio- and stereoselective metabolism of dibenz[*a*,*h*]anthracene: Identification of 12 new microsomal metabolites. *Mol. Pharmacol.* **32**, 710−722.

(38) Capdevila, J., Estabrook, R. W., and Prough, R. A. (1978) The microsomal metabolism of benzo[*a*]pyrene phenols. *Biochem. Biophys. Res. Commun.* **82**, 518−525.

(39) Bevan, D. R., and Sadler, V. M. (1992) Quinol diglucuronides are predominant conjugated metabolites found in the bile of rats following intratracheal instillation of benzo[*a*]pyrene. *Carcinogenesis* **13**, 403−407.

(40) Vigny, P., Ginot, Y. M., Kindts, M., Cooper, C. S., Grover, P. L., and Sims, P. (1980) Fluorescence spectral evidence that benzo-[*a*]pyrene is activated by metabolism in mouse skin to a diol-epoxide and a phenol-epoxide. *Carcinogenesis* **1**, 945−950.

(41) Hulbert, P. B., and Grover, P. L. (1983) Chemical rearrangement of phenol-epoxide metabolites of polycyclic aromatic hydrocarbons to quinone-methides. *Biochem. Biophys. Res. Commun.* **117**, 129−134.

(42) Wilson, N. M., Christou, M., Turner, C. R., Wrighton, S. A., and Jefcoate, C. R. (1984) Binding and metabolism of benzo[*a*]pyrene and 7,12-dimethylbenz[*a*]anthracene by seven purified forms of cytochrome P-450. *Carcinogenesis* **5**, 1475−1483.

(43) Hall, M., Forrester, L. M., Parker, D. K., Grover, P. L., and Wolf, C. R. (1989) Relative contribution of various forms of cytochrome P450 to the metabolism of benzo[*a*]pyrene by human liver microsomes. *Carcinogenesis* **10**, 1815−1821.

(44) Cavalieri, E. L., Rogan, E. G., Cremonesi, P., and Devanesan, P. D. (1988) Radical cations as precursors in the metabolic formation of quinones from benzo[*a*]pyrene and 6-fluorobenzo[*a*]pyrene. Fluoro substitution as a probe for one-electron oxidation in aromatic substrates. *Biochem. Pharmacol.* **37**, 2173−2182.

(45) Degenhardt, C., Bors, W., Stettmaier, K., Seidel, A., Frank, H., and Platt, K.-L. (1996) Metabolic activation of anthanthrene: Significance of stable radicals derived from its key metabolite 3-hydroxyanthanthrene. *Polycyclic Aromatic Compd.* **10**, 85−92.

(46) Lorentzen, R. J., Caspary, W. J., Lesko, S. A., and Ts'o, P. O. P. (1975) The autoxidation of 6-hydroxybenzo[*a*]pyrene and 6-oxobenzo[*a*]pyrene radical, reactive metabolites of benzo[*a*]-pyrene. *Biochemistry* **14**, 3970−3977.

(47) Gozukara, E. M., Guengerich, F. P., Miller, H., and Gelboin, H. V. (1982) Different patterns of benzo[*a*]pyrene metabolism of purified cytochromes P-450 from methylcholanthrene, β-naphthoflavone and phenobarbital treated rats. *Carcinogenesis* **3**, 129−133.

(48) Nemoto, N., Takayama, S., and Gelboin, H. V. (1978) Sulfate conjugation of benzo[*a*]pyrene metabolites and derivatives. *Chem.-Biol. Interact.* **23**, 19−30.

(49) Lilienblum, W., Platt, K. L., Schirmer, G., Oesch, F., and Bock, K. W. (1987) Regioselectivity of rat liver microsomal UDP-glucuronosyltransferase activities toward phenols of benzo[*a*]-pyrene and dibenz[*a*,*h*]anthracene. *Mol. Pharmacol.* **32**, 173−177.

(50) Glatt, H., Pauly, K., Frank, H., Seidel, A., Oesch, F., Harvey, R. G., and Werle-Schneider, G. (1994) Substance-dependent sex differences in the activation of benzylic alcohols to mutagens by hepatic sulfotransferases of the rat. *Carcinogenesis* **15**, 2605−2611.

TX010131T